Int J Adv Manuf Technol (2006) 31: 528–538
DOI 10.1007/s00170-005-0222-7

ORIGINAL ARTICLE

Neville K. S. Lee · Grace Yu ·
Ajay Joneja · Dariusz Ceglarek

The modeling and analysis of a butting assembly in the presence of workpiece surface roughness and part dimensional error

Received: 14 January 2005 / Accepted: 30 July 2005 / Published online: 18 March 2006

Abstract Butt joints are frequently used in assembly processes. However, relatively little attention has been paid to the proper design and selection of butt joint geometries and processes. In this paper, the assembly accuracy performance of different butt joint geometries and joining processes has been studied by using analytical models for part misalignment in the presence of part dimensional errors, surface roughness, and surface waviness. Our analysis shows that both short-term roughness, as well as long-term waviness, has an effect on the assembly precision levels. The analysis is verified statistically using a simulation program; experiments are conducted using this program to show that the differences in the performance between different butt joining methods can be significant. Therefore, proper design and selection of forming butting assemblies can have important impacts on the assembly precision.

Keywords Butt joints · Assembly precision · Surface modeling · Part dimensional error

1 Introduction

The dimensional accuracy of an assembly is important, as it can affect the quality, yield, and cost of many products. Part location errors have a significant effect on assembly accuracy. Fixtures are used to locate and hold workpieces during manufacturing operations, such as machining, assembling, and measuring. In machining, fixture designs have been analyzed in terms of their ability to arrest translation and rotation, while minimizing deflection and distortion of the part during processing. These include the effects of clamping force and sequence on workpiece dimensional accuracy [1, 2], fixture rigidity and deformation in contact surfaces between the workpiece and its locators [3–5], fixture configuration for form closure [6], fixture/locator error [7–10], and fixture configuration for force closure [11, 12]. Since fixtures form an assembly with the workpiece, there has also been research on the accuracy of assemblies based on tolerances specified on different form features or dimensions of the components. However, the above models cannot be applied to the analysis of precision butting assemblies where errors due to forces are insignificant relative to errors due to surface variations.

Ceglarek and Shi [8] classified different types of joints and developed a model to compare different joint designs. Mantipragada and Whitney [13] also analyzed tolerance stack-up in two different classifications of assemblies. Geometrical constraint propagation methods have been proposed to model the assemblies of mechanical parts and study the feasibility of a given locating sequence under the assumption that the geometry of all assembled components is known during the design process [14, 15]. These methods did not address part variability due to form errors, such as surface roughness and waviness.

The effects of such form errors on a fixtured workpiece have been partially addressed in some recent works. Sangnui and Peters [16] employed the Newton-Raphson technique to develop a mathematical model to predict the effect of surface irregularities on the location and orientations of a cylindrical workpiece. The effects of workpiece imperfections and surface roughness that affect the alignment precision of a mechanical alignment system (MAS) have been studied in the works of Lee and Joneja [17] and Lee et al. [18]. But these methods focus on part alignment with respect to a set of datums, and cannot be applied to butt joining assembly precision.

To study the level of precision for butting assemblies, it is important to have an accurate model of the geometry of the

N. K. S. Lee (✉) · G. Yu · A. Joneja
Department of Industrial Engineering and Engineering Management (IEEM), HKUST,
Clear Water Bay,
Kowloon, Hong Kong
e-mail: nlee@ust.hk
e-mail: grace@ust.hk
e-mail: jajoneja@ust.hk

D. Ceglarek
Department of Industrial Engineering,
University of Wisconsin,
Madison, WI, USA
e-mail: darek@engr.wisc.edu

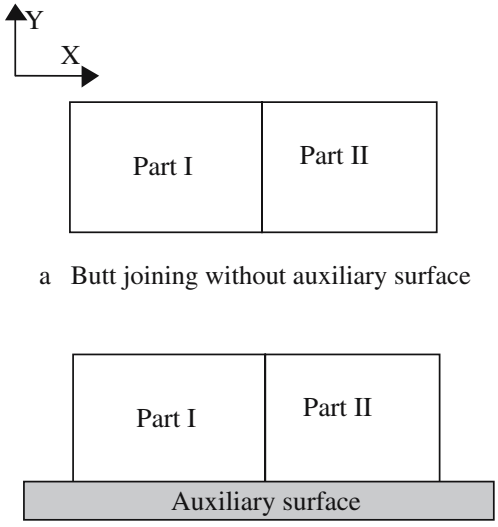

a Butt joining without auxiliary surface

b Butt joining with auxiliary surface

Fig. 1 Schematics of butt joining without and with auxiliary surface

part surface. Surface characterization is an old and important field. For instance, numerical methods have been successfully applied to generate randomly rough surfaces in the past decade. Various approaches have been used to generate two-dimensional profiles or three-dimensional surfaces with prescribed statistical properties (probability density function (PDF) and surface autocorrelation functions (ACF)). Gaussian and non-Gaussian surface profile generations with given PDFs and ACFs have been developed in [19–21] by using digital filtering techniques. In this study, a recently developed model for surfaces using autoregressive moving averages (ARMA) over short- and medium-terms and a B-spline model for waviness over long term [22] is used to model surface variations.

We address some of the gaps in the study of assembly precision in the context of butt joints. First, we develop a method to geometrically model part-to-part joint geometry in the presence of surface roughness, waviness, and part dimensional errors. Using this model, we examine assembly precision for different configurations and processes to achieve butt joints. Our simulation-based study shows that the proper design and selection of the butt joining processes can have important impacts on the assembly precision. From the analysis, we gain some important insights into the use of MASs as applied to butt joints. Currently, high-precision butt assemblies are often achieved by the use of active (e.g., using optical devices) alignment [23, 24]. This process is slow and expensive for large-scale production. A clear understanding of the effect of datum surface errors on the precision level can guide MAS system designers to choose additional preparatory machining (e.g., grinding) to bring the expected assembly accuracy to within the original specs. Secondly, MAS design itself can be made more robust, so as to suppress the effect of surface inaccuracies to some extent (some practical guidelines have been described in [17], for example).

2 Geometric consideration of butt joining processes

The schematics for simple butt assemblies, with or without an auxiliary alignment surface, are shown in Fig. 1. Figure 2 shows the two approaches that may be adopted for butt joining with an auxiliary surface. In Fig. 2a, first, workpiece 1 is aligned with the auxiliary plane; workpiece 2 is pushed downwards so that it is also aligned with the auxiliary plane before it is pushed into contact workpiece 1. An alternate approach is shown in Fig. 2b. In this approach, workpiece 2 is first pressed against workpiece 1, and then it is pushed towards the auxiliary plane along the mated surface of workpiece 1. When workpiece 2 is pushed downwards towards the auxiliary plane, the two mated workpieces are always in contact with each other.

Fig. 2 Alternate modes of achieving butting assembly

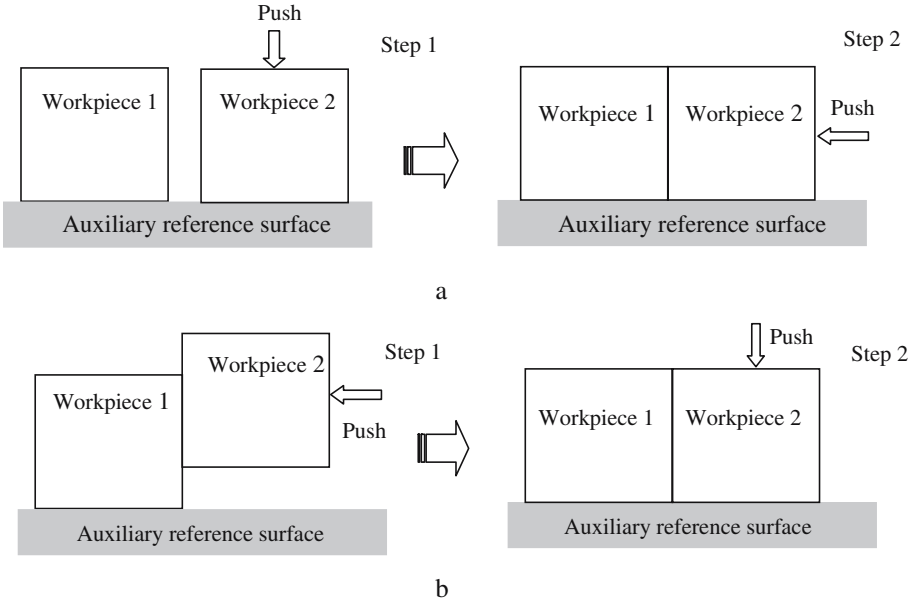

Assembly accuracy will be characterized in terms of the relative position and orientation between the mating parts. Our objective is to study the variation of distance between the actual center points of the two mated parts and the variation of orientation between these parts for different butting assembly processes in the presence of dimensional errors and surface roughness.

2.1 Impact of part dimensional error

The impact of dimensional errors on the dimensional accuracies of butt joining processes without and with an auxiliary surface is shown in Fig. 3. The ideal positions of the two assembled parts without dimensional error are represented by dotted rectangles, with the local coordinate frames shown by O_1 and O_2. The dimensional accuracies of butt joining processes depend strongly on the dimensional error of each part.

2.2 Impact of surface roughness and waviness

Figure 4 shows how surface roughness affects the dimensional accuracy for butt joining processes without an auxiliary surface, with a continuous auxiliary surface, and with discrete auxiliary surfaces. If the surface geometry is ideal, the whole surfaces will contact with each other; but in the presence of surface roughness, workpiece surfaces contact at two points. The separation between the nominal workpiece surfaces will depend on how the peaks and valleys of each surface are related to each other. For butt joining processes with an auxiliary surface, it is interesting to observe that the two scenarios produce different alignment configurations.

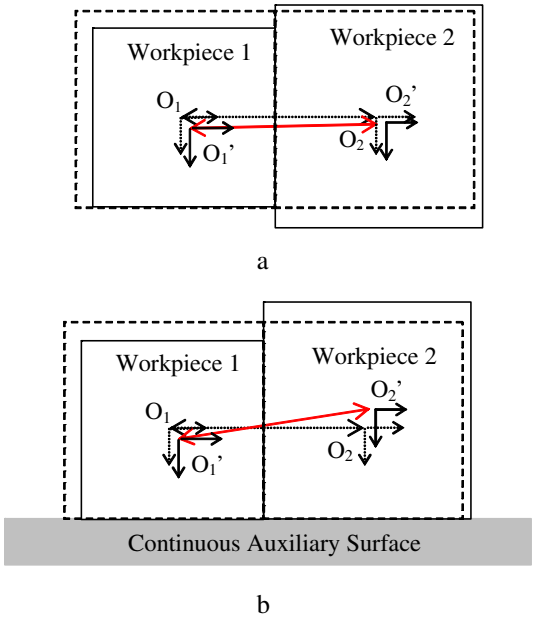

Fig. 3 a, b Impacts of part dimensional errors on the dimensional accuracies of butt joining processes: **a** without auxiliary surface; **b** with continuous auxiliary surface

For butting method 1, the contact condition for workpiece 2 is that it has two contact points with the auxiliary surface and one contact point with workpiece 1. Butting method 2 gives one contact point with the auxiliary surface and two contact points with workpiece 1. These configurations lead to different assembly accuracies. Furthermore, the dimensional accuracy that we can achieve with a continuous auxiliary surface is different from that with a discrete auxiliary surface, due to the different contact configurations between the workpieces and the auxiliary surface. For simplicity, we assume that the auxiliary surfaces are much smoother than the workpieces and ignore their surface roughness in our dimensional accuracy analysis. We denote the butt joining process without an auxiliary surface as Type 1; the process with a continuous auxiliary surface by butting method 1 as Type 2a; the process with a continuous auxiliary surface by butting method 2 as Type 2b; the process with a discrete auxiliary surface by butting method 1 as Type 3a; and the process with a discrete auxiliary surface by butting method 2 as Type 3b (Fig. 4).

Lee et al. [18] had shown that the surface roughness affects the assembly accuracy. Lee and Joneja [17] had shown the effects of global variations (called surface defects) on the assembly accuracy. However, these cases were analyzed in isolation. The discussion above makes it clear that local surface roughness (e.g., in the region where the workpiece surface contacts the datum establishing locating pin), as well as global variations (e.g., waviness), have an affect on the accuracy of butting assemblies. In this paper, a technique is developed to estimate the combined affects of both of these factors in the different modes of the butting assembly.

Our analysis requires an accurate and realistic surface model—this model is described in the next section. Using these models, it is possible to set up a simulation study that estimates the assembly accuracy in the different modes, and compares the relative merits of these approaches. A method to do so will be discussed in Sect. 4. The results from the computational model will be presented in Sect. 5. The final section discusses the findings of this study.

3 Surface modeling

Assembly inaccuracies depend on surface geometry, so it is essential to develop a complete and accurate model of the surface in order to analyze them. Both short- and long-term variations affect precision levels; a recently developed surface model with this capability is used for our study [22]. Since our analysis depends heavily on the surface model, and to make this paper self-contained, we describe it here in brief.

The surface variations are derived from a set of experimental measurements on surface profiles for different materials; multiple samples of each material were prepared using different manufacturing processes. The simplest example are aluminum samples prepared on a CNC milling machine. Short-range measurements were made using a Tencor P-10 surface profiler (horizontal resolution of 0.1 μm and vertical resolution of 1A) at three different positions on the sample with a sampling interval of 1 μm and a measurement length of 300 μm. Medium- and long-range measurements were

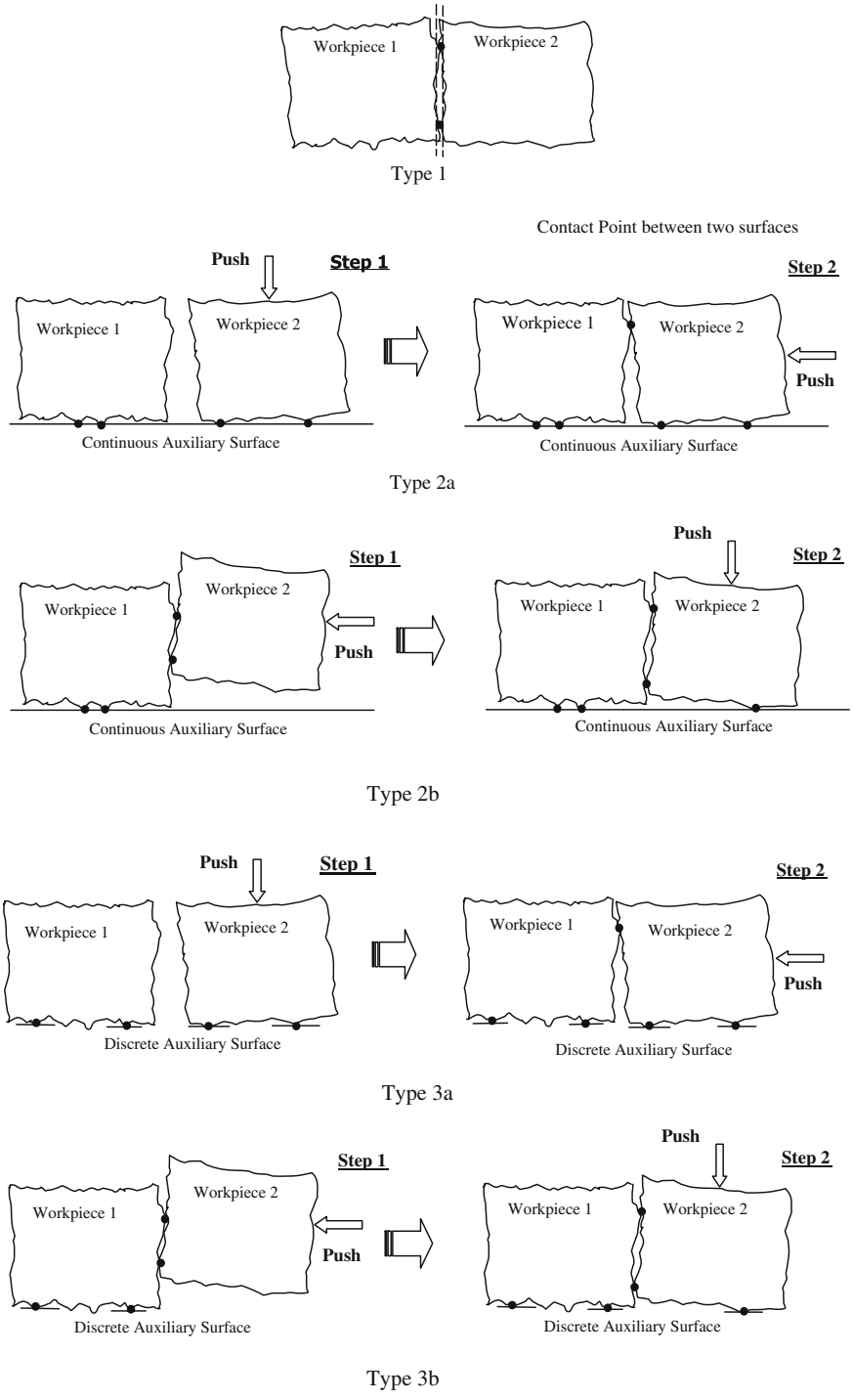

Fig. 4 Assembly errors due to surface roughness and waviness of the mated parts for five types of butt joining processes

made on an IMS coordinate measurement machine (CMM), with a sampling interval of 0.2 mm. Typical measured surface profiles of the samples are shown in Figs. 5 and 6.

The short- and medium-range profiles are characterized by four parameters: the RMS roughness σ; the correlation length, l, of the ACF that describes the spatial structure; the skewness; and the kurtosis. The long-range profiles of the samples follow simple, smooth curves with a few extreme points and are modeled by low-order polynomials.

An autoregressive integrated moving average, ARIMA (p, d, q) time series is used to generate short- and medium-range profiles for the samples as follows [25]:

$$\varphi(B)y_t = \phi(B)(1-B)^d y_t = \nabla^d \phi(B) y_t = \theta(B)a_t \qquad (1)$$

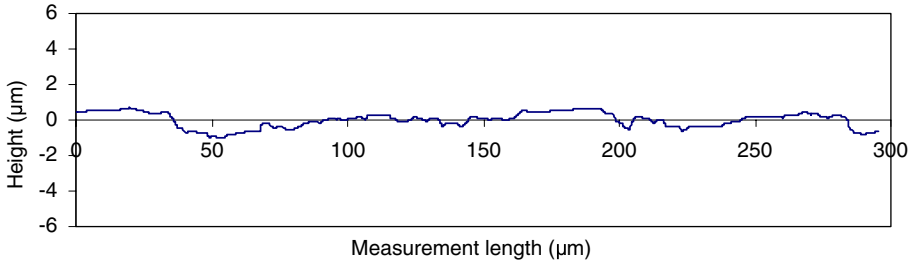

Fig. 5 Profile of milled aluminum sample measured by using a Tencor P-10 surface profiler

where B is the backward shift operator and is defined by $By_t = y_{t-1}$:

$$\phi(B) = 1 - \phi_1 B - \phi_2 B^2 \ldots - \phi_p B^p$$

$$\theta(B) = 1 - \theta_1 B - \theta_2 B^2 \ldots - \theta_q B^q$$

where $\phi(B)$ is called the autoregressive operator; $\varphi(B) = \nabla^d \phi(B)$ is the generalized autoregressive operator; $\theta(B)$ is the moving average operator; a_t is the residual white noise that is assumed to have zero mean and Gaussian or non-Gaussian distribution property; ϕ_1,..., ϕ_p, θ_1,..., θ_q are constants; and d is the differencing times.

The non-stationary data set is transformed by differencing the original data set one or more times, yielding a stationary autoregressive moving average model ARMA(p, q). Equation 1 could be rewritten for one-time differencing, d=1, as:

$$\phi(B)(y_t - y_{t-1}) = \theta(B)a_t \tag{2}$$

Since the transformed data series $\nabla y_1 = y_t - y_{t-1}$ can be generated with the ARMA model, therefore, if the starting point of y (y_0) is given, the data series y could be generated. Moreover, since y_0 only affects the average value of y in the ARIMA model, we could choose any finite value for it.

The $\phi(B)$ and $\theta(B)$ for each transformed data series is determined by standard Box-Jenkins methods [26]; a_t can be generated for the required ARMA process based on the determined $\phi(B)$ and $\theta(B)$, as well as the distribution of the transformed data series. The standard deviation, skewness, and kurtosis of residuals a_t for each ARMA model is calculated based on the relationships between the standard deviation, skewness, and kurtosis of a_t and those of the corresponding estimated ARMA process z_t given by Davies et al. [27]:

$$S_d(z) = \left(\sum_{i=0}^{\infty} C_i^2\right)^{1/2} S_d(a) \tag{3}$$

$$S_k(z) = \frac{E\left[z_t^3\right]}{\left(E\left[z_t^2\right]\right)^{3/2}} = \frac{\sum_{i=0}^{\infty} C_i^3 S_k(a)}{\left(\sum_{i=0}^{\infty} C_i^2\right)^{3/2}} \tag{4}$$

$$K(z) = \frac{E\left[z_t^4\right]}{\left(E\left[z_t^2\right]\right)^2} = \frac{\sum_{i=0}^{\infty} C_i^4}{\left(\sum_{i=0}^{\infty} C_i^2\right)^2} K(a) + \frac{\sum_{i=0}^{\infty}\sum_{j}^{\infty} C_i^2 C_j^2}{\left(\sum_{i=0}^{\infty} C_i^2\right)^2} \tag{5}$$

In Eqs. 3, 4, and 5, C_0=1; C_i ($i \neq 0$) is determined by following the equation $\phi(B)C(B) = \theta(B)$, where $C(B)$ has the form $C(B) = 1 + C_1 B + C_2 B^2 + \cdots$. Therefore, the noise terms will be generated with a standard random normal generator and then transformed into a distribution with the calculated skewness and kurtosis of a_t by employing the Johnson translatory system of distributions [28].

The long-range profiles for the same type (material, process) of samples always followed the same shape trends. The ARIMA cannot suitably capture this partial randomness. Cubic Bezier curves were found to be sufficient to capture

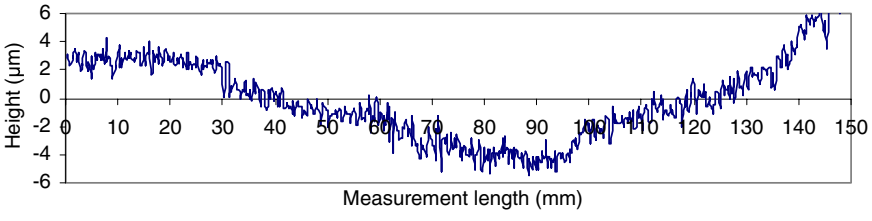

Fig. 6 Profile of milled aluminum sample measured by using a coordinate measurement machine (CMM) machine

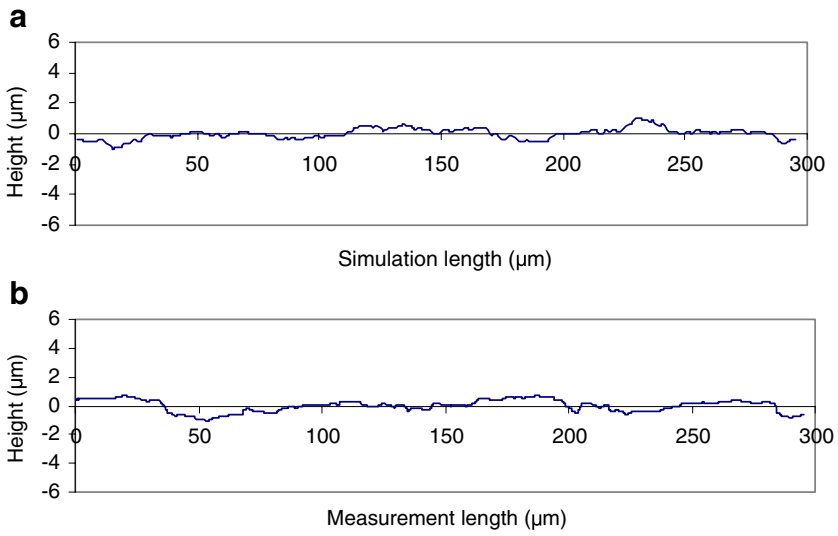

Fig. 7 **a** Simulated short-range profile of aluminum sample. **b** Measured short-range profile of aluminum sample

these trends. A Bezier curve [29] is a parametric polynomial of degree n, given in vector form as:

$$r(u) = \sum_{i=0}^{n} \frac{n!}{i!(n-i)!} u^i (1-u)^{n-i} C_i \tag{6}$$

The control points, C_i are determined by fitting the best curve over a set of k curve points, determined as follows: (i) formulate a model for the distribution of the profile y value at a fixed value of x; (ii) use the resulting distribution to generate a random value of y; (iii) use similarly generated y values at k different values of x to create coordinates of k points; (iv) select the appropriate parameter values at each point; and (v) using the computed values of point coordinates, r_j and corresponding parameter values u_j, solve the system of linear equations to derive the control points C_i.

A complete surface profile is generated by superposition, i.e., a signed addition of the short-, medium-, and long-range profile values. Figures 7, 8, 9, and 10 show a simple comparison of actual and simulated surface profiles using this model.

4 Modeling of dimensional accuracies

4.1 Location errors for different types of butt joints

Assembly positioning errors caused by workpiece dimensional error and surface roughness of mated surfaces in the first butting method for butt joining with continuous auxiliary surface is shown in Fig. 11a. In the following, to assign location errors, we fix a local coordinate frame to the (nominal) center of each workpiece. The width and height for workpieces 1 and 2 are W_1, H_1 and W_2, H_2, respectively. The dimensional errors are specified as: δW_1, δW_2 (width variation) and δH_1, δH_2 (height variation). These are computed by fitting a mean line to each edge of each workpiece. The datum surfaces are not ideal—their profile follows stochastic patterns, and, for simulation, these can be generated as

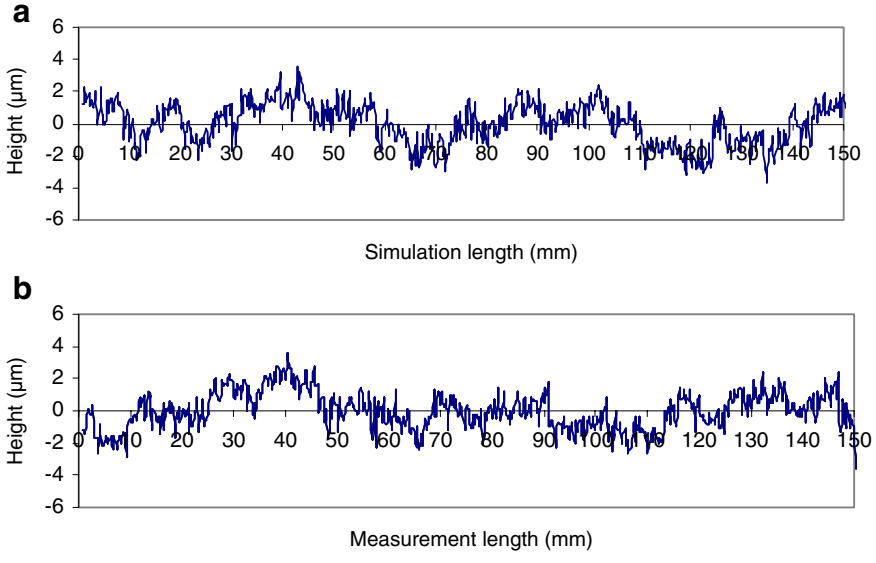

Fig. 8 **a** Simulated medium-range profile of milled aluminum sample. **b** Measured medium-range profile of 15-mm long aluminum sample

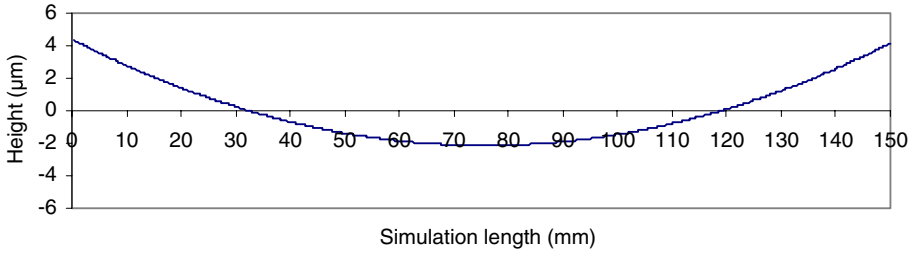

Fig. 9 Simulated long-range profile for milled aluminum sample

described earlier. Thus, each local frame will be rotated by a small angle with respect to the global frame (the global X axis is assumed to be aligned with the auxiliary surface). The angles by which workpieces 1 and 2 deviate from nominal (here, 0°) are denoted θ_1 and θ_2, respectively. These can be obtained from the simple geometric consideration of contact points (A', B', C', and D') between these two parts and the auxiliary surface, respectively. Then δ_θ, the relative orientation deviation between the two mating parts is the sum of θ_1 and θ_2. θ_1 and θ_2 are assumed to be positive when the workpiece rotates clockwise. h_1 and h_2 are the distances between the workpiece's first contact point with the auxiliary surface and the nominal surface of this workpiece along the Y direction. d_1 and d_2 are the distances between the workpiece's first contact point with the auxiliary surface and the bottom-left corner of this workpiece along the normal direction of the contacted surface on this workpiece. D is the distance between two nominal workpiece surfaces, which contact with each other, at the contact point along the X direction. In Eqs. 7 and 8, the subscripts 1 and 2 stand for workpieces 1 and 2, respectively. The location error from the ideal center-to-center distance is given by:

$$\begin{bmatrix}\delta_x\\ \delta_y\end{bmatrix} = \begin{bmatrix}\cos\theta_2 & -\sin\theta_2\\ \sin\theta_2 & \cos\theta_2\end{bmatrix}\begin{bmatrix}W_2/2-d_2\\ -H_2/2\end{bmatrix} - \begin{bmatrix}W_2/2-d_2\\ -H_2/2\end{bmatrix} - \begin{bmatrix}\cos\theta_1 & -\sin\theta_1\\ \sin\theta_1 & \cos\theta_1\end{bmatrix}\begin{bmatrix}W_1/2-d_1\\ -H_1/2\end{bmatrix} + \begin{bmatrix}W_1/2-d_1\\ -H_1/2\end{bmatrix} + \begin{bmatrix}D\\ h_1-h_2\end{bmatrix} + \begin{bmatrix}(\delta W_1+\delta W_2)/2\\ (\delta H_1-\delta H_2)/2\end{bmatrix} \tag{7}$$

$$\delta_\theta = \theta_1 + \theta_2 \tag{8}$$

where δ_x and δ_y are the deviation of distances of the two mating part center points from the ideal case with respect to the global X and Y directions, respectively.

Similarly, the assembly positioning error caused by workpiece dimensional error and surface roughness of mated surfaces for the butt joining with a continuous auxiliary surface using the second butting method is shown in Fig. 11b. We use the same notation as the first butting process model; d_2 is the distance between workpiece 2's first contact point with workpiece 1 and the upper-left corner of workpiece 2 along the nominal direction of the mated surface on workpiece 2. In this case, the location error is given by:

$$\begin{bmatrix}\delta_x\\ \delta_y\end{bmatrix} = \begin{bmatrix}\cos\theta_2 & -\sin\theta_2\\ \sin\theta_2 & \cos\theta_2\end{bmatrix}\begin{bmatrix}W_2/2\\ H_2/2-d_2\end{bmatrix} - \begin{bmatrix}W_2/2\\ H_2/2-d_2\end{bmatrix} - \begin{bmatrix}\cos\theta_1 & -\sin\theta_1\\ \sin\theta_1 & \cos\theta_1\end{bmatrix}\begin{bmatrix}W_1/2-d_1\\ -H_1/2\end{bmatrix} + \begin{bmatrix}W_1/2-d_1\\ -H_1/2\end{bmatrix} + \begin{bmatrix}D\\ h_1-h_2\end{bmatrix} + \begin{bmatrix}(\delta W_1+\delta W_2)/2\\ (\delta H_1-\delta H_2)/2\end{bmatrix} \tag{9}$$

$$\delta_\theta = \theta_1 + \theta_2 \tag{10}$$

Here, θ_2 depends on the contact points C' and D' between two workpieces instead of the contact points between workpiece 2 and the auxiliary surface.

For the two cases of butt joining with discrete auxiliary surfaces, the equations are the same as for continuous auxiliary surfaces. However, the variations of δ_x, δ_y, and δ_θ can be quite different, even for the same pair of mated surfaces, since some of the potential contact points between the parts and the continuous auxiliary surface will not be considered when using the discrete auxiliary surface.

The assembly positioning error for butt joining without auxiliary surfaces in the presence of part dimensional error and surface roughness is shown in Fig. 11c. The error in the location is given by:

$$\delta_x = (\cos\theta_2 - 1)\bullet W_2/2 - (-\sin\theta_2 - 1)\bullet (H_2/2 - d_2) + D + (\delta W_1 + \delta W_2)/2 \tag{11}$$

$$\delta_\theta = \theta_2 \tag{12}$$

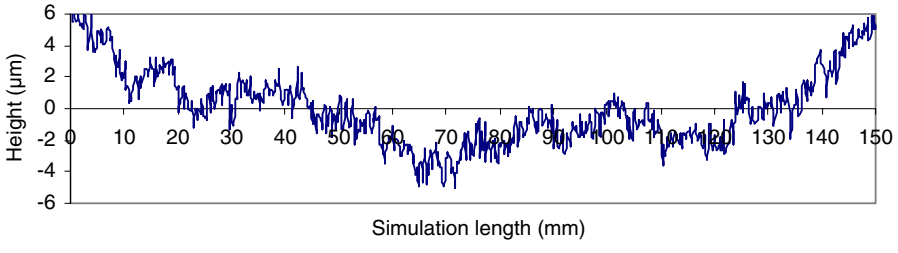

Fig. 10 Superposed long- and medium-range profiles

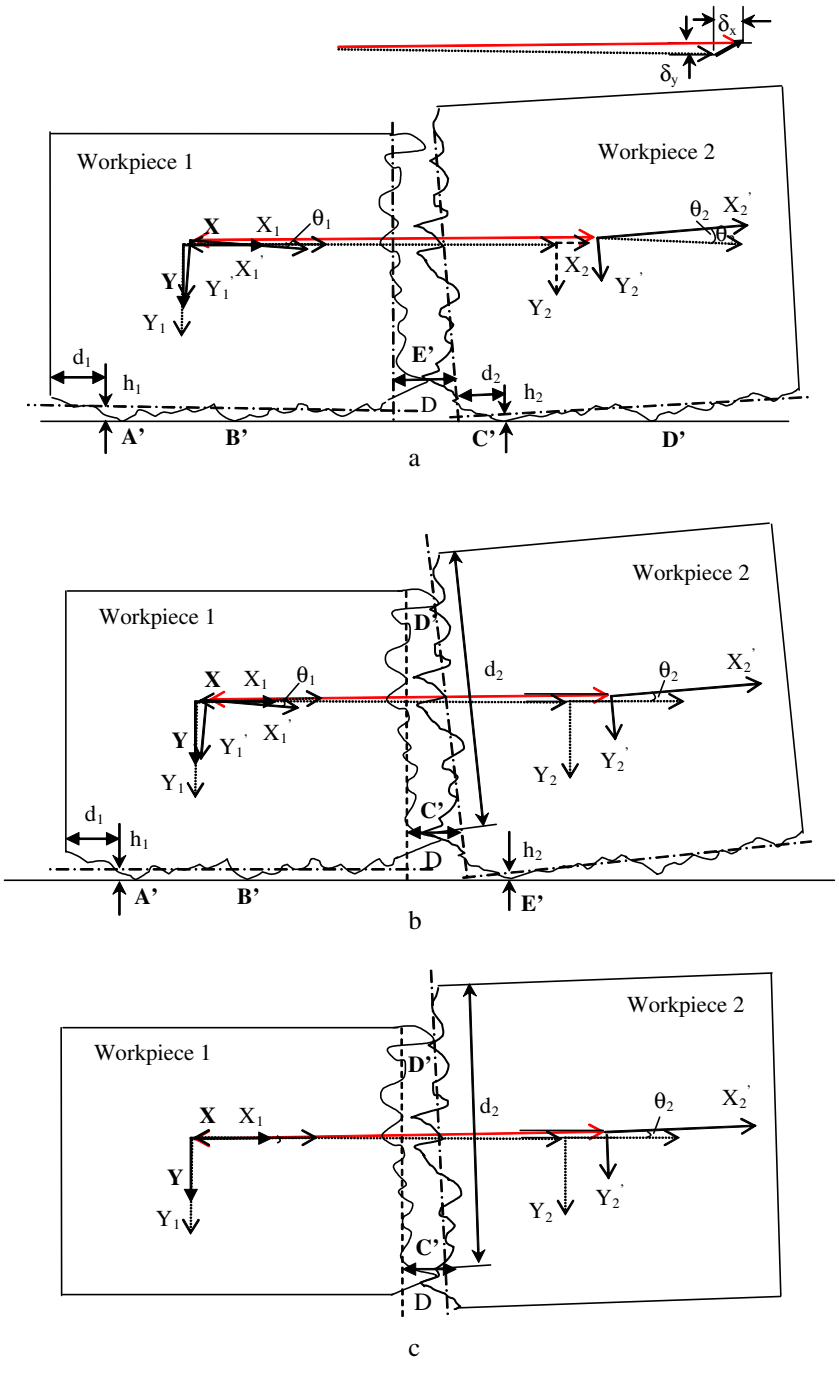

Fig. 11a–c Assembly error caused by workpiece dimensional error and surface roughness for butt joining: **a** with a continuous auxiliary surface using butting method 1; **b** with a continuous auxiliary surface using butting method 2; **c** without an auxiliary surface

5 A simulation model to study butting assembly accuracy

The effects of part dimensional error, surface waviness, and roughness are considered. Since these effects can be treated as statistically independent due to the random nature of the surface, the overall assembly variation could be expressed as follows:

$$\begin{aligned}\sigma_x &= \sqrt{\sigma_{dx}^2 + \sigma_{sx}^2}\\ \sigma_y &= \sqrt{\sigma_{dy}^2 + \sigma_{sy}^2}\\ \sigma_\theta &= \sqrt{\sigma_{d\theta}^2 + \sigma_{s\theta}^2}\end{aligned} \tag{13}$$

where $(\sigma_x, \sigma_y, \sigma_\theta)$ is the overall assembly variation; $(\sigma_{dx}, \sigma_{dy}, \sigma_{d\theta})$ is the variation due to part dimensional error; and $(\sigma_{sx}, \sigma_{sy}, \sigma_{s\theta})$ is the variation due to surface waviness and roughness. We could observe that the variation caused by part dimensional error could be easily obtained based on the geometry consideration (Fig. 3). Therefore, we will mainly concentrate on the analysis of the assembly variation due to surface waviness and roughness. As surface profiles are highly random in nature, one way to explore how surface roughness and waviness may affect the assembly precision is by using simulation. In this section, we will first discuss how to set up the simulation program and then how to generate the random surface for the workpiece.

5.1 Simulation program

A flow chart of our simulation of dimensional accuracy in the presence of part variation, surface roughness, and waviness for various butt joining processes is shown in Fig. 12. The dimensional accuracy is estimated when batches of workpieces 1 and 2 are aligned against each other with an auxiliary surface or fixture/locator and then assembled together. Input from two workpieces' part dimensional tolerance and parameters for generating mated surfaces are entered first.

In the first method for butt joining with an auxiliary surface, the auxiliary surface is used to pre-align the two workpieces. Two contact points between the auxiliary surface and each workpiece are determined, and the mated vertical surfaces of the two workpieces are recalculated. Therefore, we can find a contact point for the mated vertical surfaces of two workpieces when we push workpiece 2 towards workpiece 1. The relationship between the two center points and the relative orientation between the two parts is calculated. This process continues until enough runs have been obtained to determine the variance of relative positions between these two particular sets of workpieces.

When using the second method for butt joining with an auxiliary surface, the auxiliary surface is first used to pre-

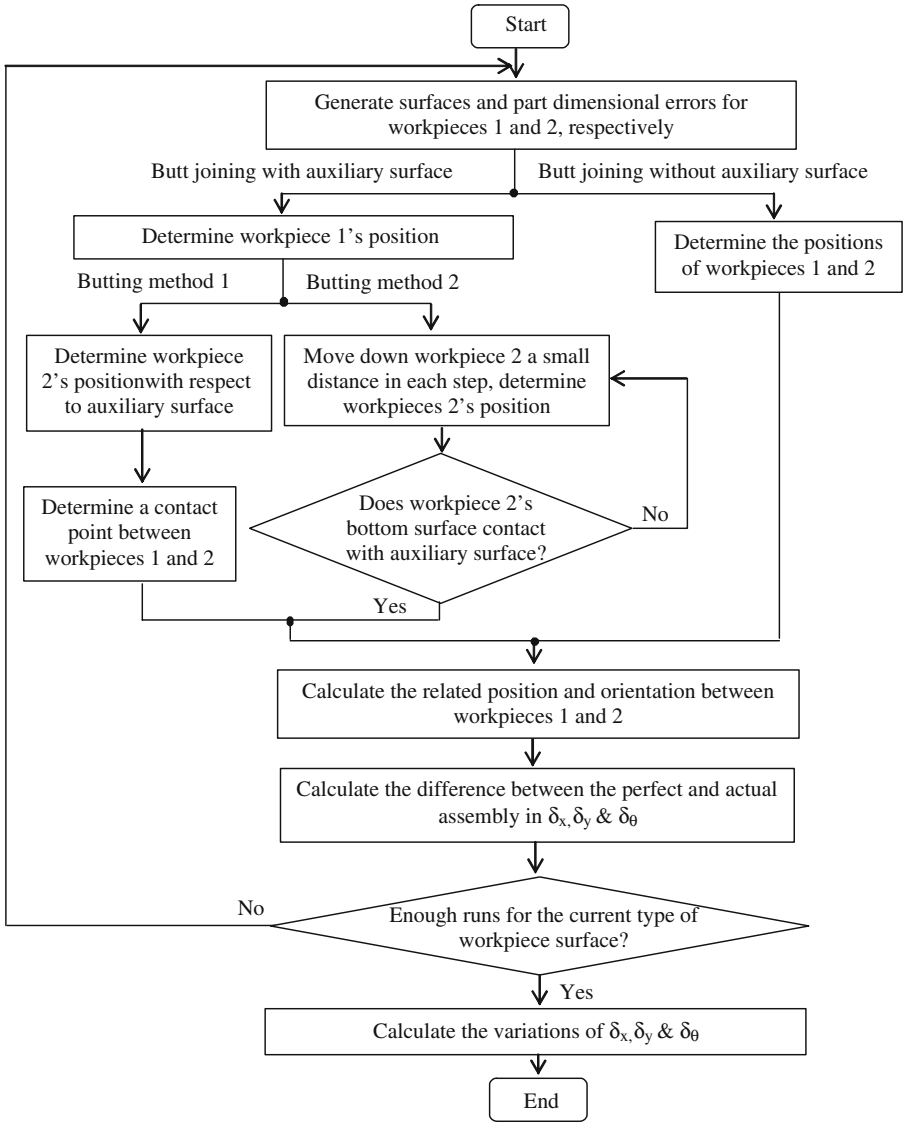

Fig. 12 Simulation flow chart diagram of dimensional accuracy in the presence of part variation and surface roughness for butt joining with and without an auxiliary surface

Table 1 Assembly variations for butt joints with no auxiliary surface

Workpiece dimensional error (μm)	Dimensional variation			
	150-mm long aluminum sample		150-mm long plastic sample	
	σ_θ (μrad)	σ_x (μm)	σ_θ (μrad)	σ_x (μm)
0	22.8846	3.1934	169.5921	7.9515
250	22.8846	176.8344	169.5921	177.1340
500	22.8846	353.5822	169.5921	353.7322

align workpiece 1. Two contact points with the auxiliary surface are determined and the right vertical surface is recalculated for workpiece 1. Workpiece 2 is lifted up for a small distance and pressed against workpiece 1 along the right vertical surface of workpiece 1. Two contact points between workpieces 1 and 2 are calculated, and the bottom surface profile of workpiece 2 is generated according to the present position of workpiece 2. Then, workpiece 2 moves down a fraction of a distance, while keeping the two contact points with workpiece 1. The whole procedure is repeated until the lowest point on the bottom surface of workpiece 2 reaches the auxiliary surface. The relationship between the two mated workpiece center points and the relative orientation between the two parts is calculated. This process continues until enough runs have been obtained to determine the variance of relative positions between these two particular sets of workpieces. The procedure for discrete auxiliary surfaces is similar, except that we ignore the potential contact points that do not contact with the discrete auxiliary surfaces between the parts and the auxiliary surface, and continue to search until we have the required number of contact points between the parts and the discrete auxiliary surfaces.

For the simulation of dimensional accuracy for butt joining without an auxiliary surface, two contact points are determined and the relationship between the two center points of the two workpieces along the X direction and the relative orientations of the two parts are calculated.

5.2 Simulation results

In the simulation study, profiles of several samples of two types of materials, plastic and aluminum, were generated based on measured surface characteristics. All samples were 150-mm long. For the aluminum samples, a mean short-range roughness range was 1.9 μm, while the waviness range over the entire length was 10.8 μm. The corresponding values for the plastic samples were 8.8 μm and 45.7 μm. The measurements were made on datum surfaces prepared by down milling using a 10-mm HSS tool fixtured on a DYNA CNC mill at a spindle speed of 2,350 rpm, 20 cm/min federate, and a depth of cut of 0.1 mm per pass. The surface measurements were made using a Tencor P-10 surface profiler and a Mitutoyo CMM. The simulation results of the assembly variations for butt joints due to surface waviness and roughness are shown in Tables 1 and 2. In the tables, σ_{sx}, σ_{sy}, and $\sigma_{s\theta}$ represent the one-sigma variation of relative position in the X and Y directions and variation of the relative orientations for the two mated parts due to surface waviness and roughness.

It is not surprising to note that the accuracy of the butt joints depends heavily on the dimensional variations. Further, we consider the effects of roughness and waviness using the cases by setting the dimensional error to 0 μm. The results show that the selection of butt joint geometries and joining processes can substantially affect the assembly precision of butt joints. Different butt joint geometries and joining processes have their own merits, as some processes may provide better assembly precision along different directions. For the two butting processes with continuous auxiliary surfaces, one process has a relatively higher dimensional accuracy in the butting direction, while the other process has a relatively higher dimensional accuracy in the direction normal to the butting direction. The assembly variation of one process could be as high as four times that of the assembly variation of the other process in one direction. We also notice that the butting process with a discrete auxiliary surface, which may have a relatively higher dimensional accuracy than the process with a continuous auxiliary surface under some situations (e.g., when the workpiece surfaces are totally random), is not suitable for improving the joint dimensional accuracy in our study, due to our particular workpiece surface profiles that have certain repeatable patterns (i.e., partially random long-range profile components). This can be explained as follows: when we adopt the continuous auxiliary surfaces, the two contact points between the workpiece and the auxiliary surfaces are always within certain areas of the workpiece surfaces (e.g., the two contact points between the aluminum sample surface and the continuous auxiliary surface happen at both surface ends). However, the distance between these two contact points will be shortened when adopting the discrete auxiliary surfaces. This may lead to a

Table 2 Assembly variations for butt joints with an auxiliary surface (refer to Fig. 2)

Butting method	Workpiece dimensional error (μm)	Dimensional variation of joint					
		150-mm long aluminum sample			150-mm long plastic sample		
		σ_θ (μrad)	σ_x (μm)	σ_y (μm)	σ_θ (μrad)	σ_x (μm)	σ_y (μm)
1	0	29.508	3.5559	2.562	151.2114	9.6562	5.2446
	250	29.508	176.8482	176.8138	151.2114	177.3034	176.9322
	500	29.508	353.5892	353.5720	151.2114	353.8170	353.6312
2	0	23.3848	3.6689	4.5595	149.8172	9.8960	25.4745
	250	23.3848	176.8528	176.8943	149.8172	177.3298	180.4104
	500	23.3848	353.5915	353.6122	149.8172	353.8303	355.3842

larger rotation of the workpiece with respect to its ideal orientation, hence, cause worse dimensional accuracy in the butting and non-butting directions.

6 Conclusions

In this study, we confirm that part dimensional error and surface roughness have significant effects on the integrity of part-to-part joint geometry. Our study shows that different butt joint geometries and joining processes have its own merits, as some of the processes may provide better assembly precision in one direction, while the others may provide better assembly precision in the other directions. To obtain high precision in the X direction, joining without an auxiliary surface could be chosen; to obtain high precision in the Y direction, butt-to-butt joint with a discrete auxiliary surface could be chosen. Similar orientation variation could be achieved for all these part-against-part joints, except butt-to-butt joint with a discrete auxiliary surface, which causes almost three times the variation compared with the other methods. Therefore, proper design and selection of the butt joining processes can have important impacts on the assembly precision.

Acknowledgements This research was partially supported by an RGC-CERG (Project no. HKUST 6224/01E) from UGC, Hong Kong, and the US State of Wisconsin's IEDR Program, USA.

References

1. Bazrov BM, Sorokin AI (1982) The effect of clamping sequence on workpiece mounting accuracy. Sov Eng Res 2 (10):92–95
2. Cogun C (1992) The importance of the application sequence of clamping forces on workpiece accuracy. J Eng Ind 114: 539–543
3. Shawki GSA, Abdel-Aal MM (1965) Effect of fixture rigidity and wear on dimensional accuracy. Int J Mach Tool Des Res 5:183–202
4. Shawki GSA, Abdel-Aal MM (1965) Rigidity considerations in fixture design—contact rigidity at locating elements. Int J Mach Tool Des Res 6:31–43
5. Shawki GSA, Abdel-Aal MM (1966) Rigidity considerations in fixture design—rigidity of clamping elements. Int J Mach Tool Des Res 6:207–220
6. DeMeter EC (1994) The min–max load criteria as a measure of machining fixture performance. J Eng Ind 116:500–507
7. Rong Y, Li W, Bai Y (1995) Locating error analysis for computer-aided fixture design and verification. In: Proceedings of the International Computers in Engineering Conference and the ASME Database Symposium, Boston, Massachusetts, September 1995, pp 825–832
8. Ceglarek D, Shi J (1995) Dimensional variation reduction for automotive body assembly. Manufact Rev 8(2):139–154
9. Ceglarek D, Shi J (1996) Fixture failure diagnosis for the autobody assembly using pattern recognition. J Eng Ind 118 (1):55–66
10. Choudhuri SA, DeMeter EC (1999) Tolerance analysis of machining fixture locators. J Manufact Sci Eng 121:273–281
11. Lee SH, Cutkosky MR (1991) Fixture planning with friction. J Eng for Ind 113:320–327
12. Wu NH, Chan KC, Leong SS (1995) A general frictional model for fixturing verification. In: Proceedings of the 3rd International Conference on Computer Integrated Manufacturing (ICCIM'95), Singapore, July 1995, vol 2, pp 1183–1199
13. Mantripragada R, Whitney DE (1999) Modeling and controlling variation propagation in mechanical assemblies using state transition models. IEEE Trans Robotic Autom 15:124–140
14. Kramer GA (1992) A geometric constraint engine. Artif Intell 58(1–3):327–360
15. Anantha R, Kramer GA, Crawford RH (1996) Assembly modelling by geometric constraint satisfaction. Comput Aided Design 28(9):707–722
16. Sangnui S, Peters F (2001) The impact of surface errors on the location and orientation of a cylindrical workpiece in a fixture. J Manufact Sci Eng 123:325–330
17. Lee N, Joneja A (1997) A method to improve manufacturing precision in the presence of workpiece imperfections. J Manufact Sci Eng 119:616–622
18. Lee NKS, Chen JY, Joneja A (2001) Effects of surface roughness on multi-station mechanical alignment process. J Manufact Sci Eng 123:433–444
19. Oh Y (1997) Precise estimation of surface roughness parameters from field-measured ground truth data. In: Proceedings of the IEEE International Geoscience and Remote Sensing Symposium (IGARSS'97), Singapore, Aug 1997, vol 2, pp 708–710
20. Wu SC, Chen MF, Fung AK (1988) Non-Gaussian surface generation. IEEE Trans Geosci Remote Sens 26(6):885–888
21. Hu YZ, Tonder K (1992) Simulation of 3-D random surface by 2-D digital filter and Fourier analysis. Int J Mach Tools Manufact 32(1–2):83–90
22. Lee NKS, Yu G, Joneja A (2004) Surface generation spanning the short-range to long-range using time series modeling. Int J Mach Tools Manufact (in press)
23. Holcombe RS, Hoffman AW, Love PJ (2004) Mosaic packaging for large-format infrared devices. Proc SPIE 5499 (1):526–529
24. He X, Wei Z-H, Hao Z-H (2003) Digital camera modeling of butting 9 CCD chips in the concentric spherical lens system. Optic Precis Eng 11(4):421–424
25. Brockwell PJ, Davis RA (1991) Time series: theory and methods, 2nd edn. Springer, Berlin Heidelberg New York
26. Box GEP, Jenkins GM (1976) Time series analysis: forecasting and control, 2nd edn. Holden-Day, San Francisco, California
27. Davies N, Spedding TA, Watson W (1980) Autoregressive moving average processes with non-normal residuals Time Series Anal 1(2):103–109
28. Hill ID, Hill R, Holder RL (1976) Fitting Johnson curves by moments. Appl Stat 25:180–189
29. Piegl LA, Tiller W (1995) The NURBS book. Springer, Berlin Heidelberg New York